European Journal of Medicinal Chemistry 45 (2010) 4113–4121

Contents lists available at ScienceDirect

European Journal of Medicinal Chemistry

journal homepage: http://www.elsevier.com/locate/ejmech

Original article

Synthesis and biological evaluation of novel 2,4′-bis substituted diphenylamines as anticancer agents and potential epidermal growth factor receptor tyrosine kinase inhibitors

Sahar Mahmoud Abou-Seri*

Department of Pharmaceutical Chemistry, Faculty of Pharmacy, Cairo University, Kasr El-Aini street, Cairo, P.O. Box, 11562, Egypt

ARTICLE INFO

Article history:
Received 8 March 2010
Received in revised form
8 May 2010
Accepted 31 May 2010
Available online 9 June 2010

Keywords:
2,4′-Bis substituted diphenylamine derivatives
EGFR tyrosine kinase inhibitors
Antitumor
Docking

ABSTRACT

Four new series of 2,4′-bis diphenylamine hydrazones **14**, 2,4′-bis aminothiadiazole **16**, 2,4′-bis mercaptotriazole **17**–**18** and 2,4′-bis mercapto-oxadiazole diphenylamine derivatives **19**–**20** were synthesized and evaluated for their ability to inhibit EGFR tyrosine kinase. Compound *N*-ethyl-5-{2-[4-(5-(ethylamino)-1,3,4-thiadiazol-2-yl)- phenylamino]phenyl}-1,3,4-thiadiazol-2-amine **16a** was the most active enzyme inhibitor (98% inhibition at 10 μM). Moreover, all compounds that showed enzyme inhibition activity were tested in vitro on human breast carcinoma cell line (MCF-7) in which EGFR is highly expressed. The tested compounds exploited potent antitumor activity with IC_{50} values ranging 0.73–2.38 μM. Molecular modeling and docking of the synthesized compounds into the active site of EGFR kinase domain showed good agreement with the obtained biological results. The present work represents a novel class of diphenylamine based derivatives with potent cytotoxicity and promising EGFR PTK inhibition activity.

1. Introduction

The ErbB or epidermal growth factor (EGF) receptors are members of subclass 1 of the protein tyrosine kinase (PTK) super family. There are four ErbB receptor family members: ErbB1 (EGFR, HER1), ErbB2 (HER2/neu), ErbB3 (HER3), ErbB4 (HER4) [1–4]. The receptors are situated at the cell membrane and have an extracellular ligand binding domain, a transmembrane domain and a cytoplasmic tyrosine kinase domain. Ligand binding to the receptors results in receptor homo- and hetero-dimers, activation of the intrinsic kinase domain and phosphorylation of specific tyrosine residues within the cytoplasmic tail. Protein dock on these phosphorylated residues, leads to the activation of a variety of intracellular signaling pathways that promote cell growth, proliferation, differentiation, survival and migration [1–4]. Overexpression of EGFR and ErbB2 has been associated with aggressive diseases and poor prognosis in range of human tumors (e.g. breast, lung, ovarian and squamous carcinoma of head and neck) [5–7]. The EGFR signaling is important for tumor cell proliferation, inhibition of apoptosis, angiogenesis, metastasis and sensitivity to chemotherapy and radiotherapy [8]. Therefore, inhibition of EGFR signaling may not only has an antiproliferative and therapeutic effects but also increases sensitivity to cytotoxic therapies [9].

Various approaches have been developed to target the ErbB signaling pathways including: 1) Monoclonal antibodies like trastuzumab and cetuximab directed against the receptor [10,11]; 2) ATP-competitive small molecule inhibitors of the intrinsic tyrosine kinase domain like geftinib **1** and erlotinib **2** [12]. Lapatinib **3** is a potent dual EGFR/ErbB2 inhibitor, recently approved for treatment of breast cancer [13]. These agents belong to the class of 4-anilinoquinazoline (Fig. 1). Although the ATP binding site shows high homology with other ATP driven receptor kinases, 4-anilinoquinazolines have been proved as selective potent inhibitors of EGFR binding site [14–18]. The quinazoline moiety fits into the ATP-binding pocket in the kinase domain, while the aniline ring fills an adjacent lipophilic pocket [19]. Since, 4-anilinoquinazolines have very tight structure activity relationship, this emerged the need to develop non-quinazoline EGFR inhibitors.

Hodge and Pierce revealed a bioisosteric relationship between salicylic group and quinazoline. They suggested that the hydrogen bond array of salicylamide could mimic the prymidine ring of quinazolines [20]. Later, different salicylanilides **4** have been reported as potent inhibitors of EGFR PTKs. This led to the hypothesis, that salicylanilides may adopt the same binding mode to EGFR PTK as quinazolines [21,22]. Moreover, 4-amino-6-arylaminopyrimidine-5-carbalehyde oximes **5** and 5-carbalehyde

* Tel.: +2 02 25591683; fax: +2 02 2362 8426.
E-mail address: saharshaarawy_69@yahoo.com

0223-5234/$ – see front matter © 2010 Elsevier Masson SAS. All rights reserved.
doi:10.1016/j.ejmech.2010.05.072

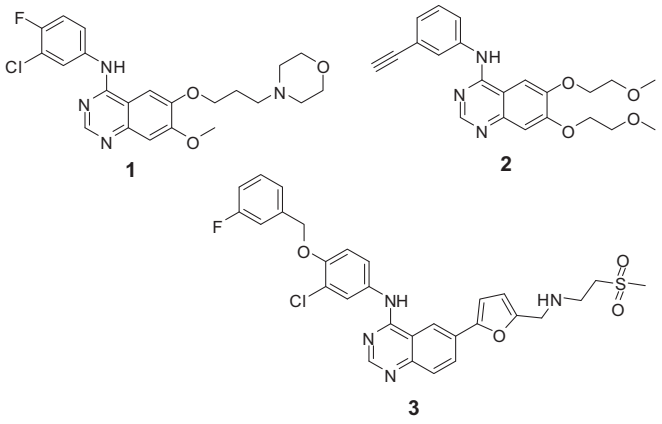

Fig. 1. 4-Anilinoquinazolines EGFR-TK inhibitors, Gefitinib **1**, Erlotinib **2**, Lapitinib **3**.

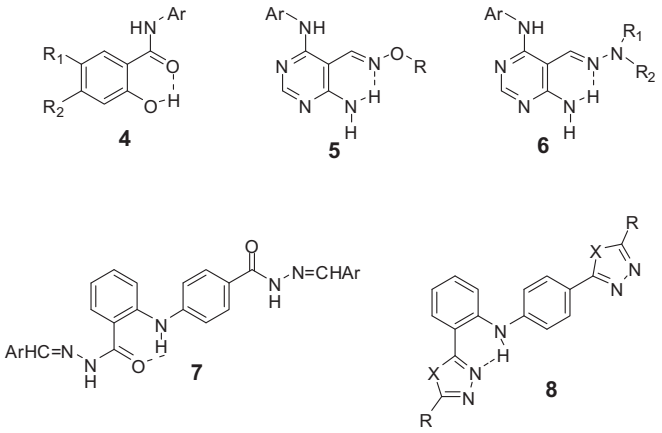

Fig. 2. Salicylanilides **4**, carbaldehyde 5-oxime **5**, carbaldehyde 5-hydrazone **6**, 2,4′-bis substituted diphenylamine arylidene hydrazides template **7**, 2,4′-bis-heterocyclic substituted diphenylamines template **8** (X = S, N or O).

hydrazones **6** with dual EGFR/ErbB2 inhibitory properties have been reported to inhibit tumor cell proliferation of breast carcinoma in vitro [23,24]. These scaffolds effectively mimic the quinazoline kinase template by forming pseudo-bicyclic structure with the help of an intramolecular hydrogen bond (Fig. 2). In addition, diphenylamine derivatives have been evaluated as orally active antiproliferative agents that inhibit tyrosine kinase autophosphorylation [25]. Also, hydrazones have been well acknowledged to possess anticancer activity. Based on this knowledge, a series of 2,4′-bis substituted diphenylamine arylidene hydrazides **7** was synthesized. Such substitution pattern could target different regions of the ATP binding site. The pseudo six-membered ring formed by intramolecular hydrogen bond between the diphenylamine NH and 2-hydrazide Oxygen (NH…O=C) would function to mimic the pyrimidine ring of quinazolines. On the other hand, the 2-bulky substituent would interact deeply with an adjacent hydrophobic pocket present in EGFR PTK. Moreover, the 4′-substituent was expected to orient toward the solvent front, so that the produce interaction might gain an additional potency.

A number of reports have shown that fused tricyclic quinazoline analogs as pyrrolo-, pyrazolo- and imidazo-quinazolines were very potent EGFR PTKs inhibitors [26,27]. A large number of thiadiazole, triazole and oxadiazole based compounds have been shown to

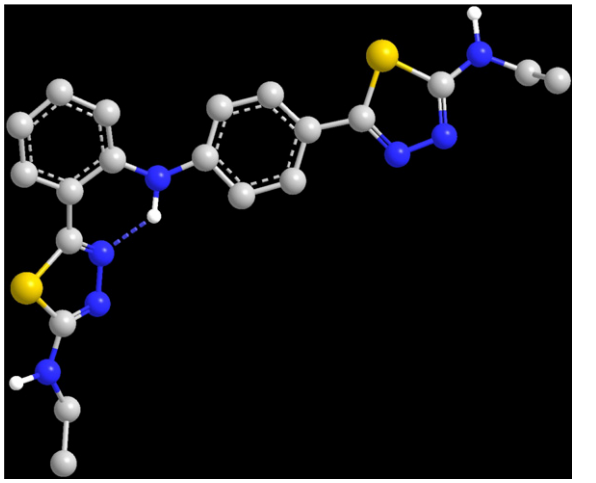

Fig. 3. Energy minimized structure of compound **16a**, showing hydrogen bonding between diphenylamine NH and N3 of thiadiazole ring.

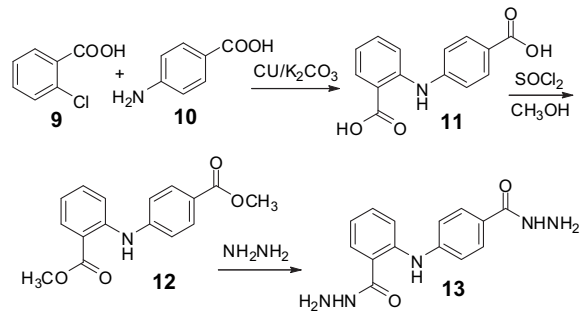

Scheme 1. Synthetic pathway for the intermediates **12**–**13**.

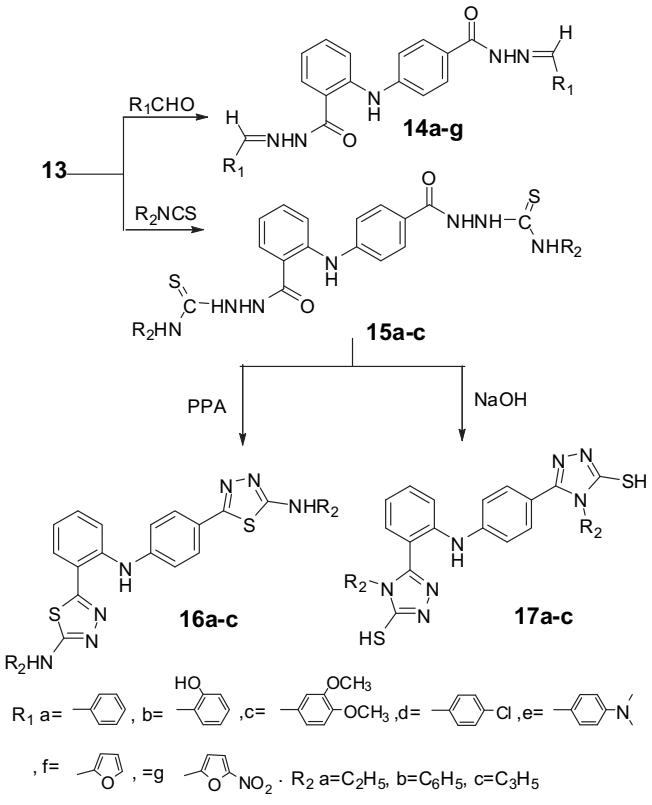

Scheme 2. Synthetic pathway for compounds **14**–**17**.

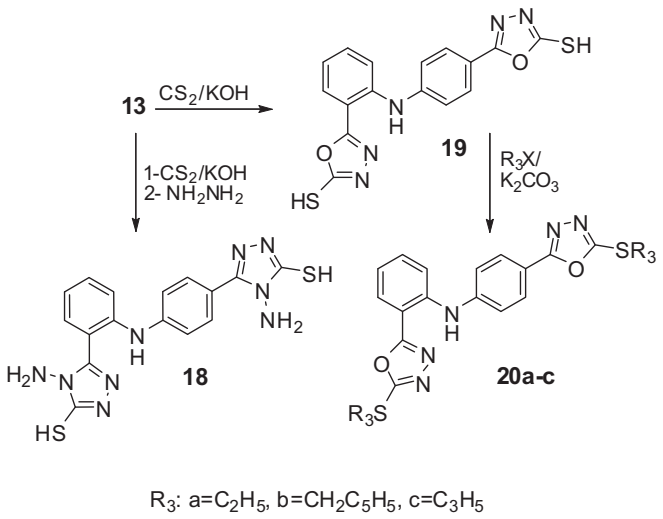

Scheme 3. Synthetic pathway for compounds **18**–**20**.

exhibit antitumor activity against a wide variety of tumor cell lines [28–31]. Therefore, different bis substituted 2,4′-diphenylamines **8** were synthesized to explore the effect of incorporating various heterocyclic bioisosters as 1,3,4-thiadiazole, 1,2,4-triazole or 1,3,4-oxdiazole ring substituents on the diphenylamine core. Such heterocyclic rings are capable of hydrogen bonding with the diphenylamine NH and would mimic a pseudo fused tricyclic quinazoline system (Figs. 2 and 3).

The present work reports the synthesis, EGFR inhibitory properties and in vitro antitumor activity against MCF-7 (breast) cell line of some 2,4′-bis substituted diphenylamines. This work represents an attempt to find new structural type of tyrosine kinase inhibitors that target EGFR.

2. Chemistry

2-{[4-(Methoxycarbonyl)phenyl]amino}benzoic acid methyl ester **12** was obtained through esterification of 2,4′-dipenylamine dicarboxylic acid **11**, obtained in turn through the condensation of 2-chlorbenzoic acid **9** and p-amino benzoic acid **10** under Ullmann condition [32]. The key intermediate 2-[4-(hydrazinecarbonyl) phenylamino] benzoic acid hydrazide **13** was prepared by hydrazinolysis of the diester **12**. Condensation of the dihydrazide **13** with different aldehydes afforded the hydrazones **14a**–**g**, while reaction with the appropriate isothiocyanate produced the thiosemicarbazides derivatives **15a**–**c**. Compounds **16a**–**c** were prepared by cyclodehydration of the corresponding thiosemicarbazides **15a**–**c** with polyphosphoric acid. Alternatively, the thiosemicarbazides **15a**–**c** were cyclized into the corresponding 1,2,4-triazol-5-thiones **17a**–**c** upon reflux with 2 N sodium hydroxide solution. On the other hand the method of Reid and Heindel was adopted for the synthesis of the 4-amino-5-mercapto-1,2,4-triazole derivative **18** [33]. Finally, the intramolecular cyclization of the diacid hydrazide **13** with carbon disulfide in presence of sodium hydroxide, produced the 5-mercapto-1,3,4-oxadiazole derivative **19**, which was alkylated with different alkyl halides in presence of potassium carbonate to yield compounds **20a**–**c**. The reaction sequences are illustrated in Schemes 1–3.

Table 1
EGFR tyrosine kinase inhibitory activity of the synthesized compounds at 10 μM.

Compound	Inhibitory activity [%] at 10 μM
14a	0.4
14b	1.2
14c	47.1
14d	2.4
14e	50.0
14f	0.8
14g	1.7
16a	97.7
16b	0.0
16c	0.0
17a	52.0
17b	0.0
17c	0.0
18	0.0
19	48.0
20a	3.4
20b	49.0
20c	50.0
Lapatinib	99.2

Table 2
In vitro cytotoxic activities of the synthesized compounds against human breast cancer cell (MCF-7).

Compound	Cytotoxicity IC_{50} (μmol)
14c	0.81
14e	1.23
16a	0.94
17a	2.38
19	2.00
20b	0.73
20c	1.05

3. Results and discussion

3.1. In vitro EGFR kinase inhibitory properties

Kinase inhibitory activity of all final compounds in Scheme 2 and 3 were evaluated using EGFR kinase activity assay by ELISA [34]. The assay was based on the inhibition of the phosphorylation of poly glutamic acid/tyrosine [Poly (Glu/Tyr), 4:1] by EGFR tyrosine kinase. Results are summarized in Table 1. The inhibitory activities

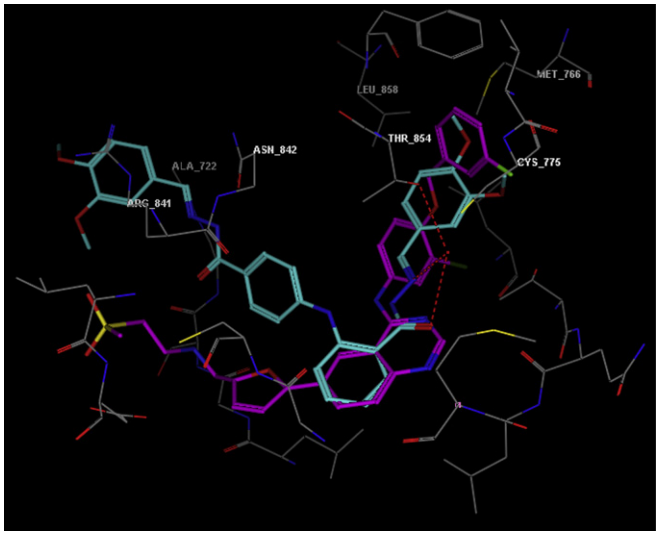

Fig. 4. The superposition of lapatinib (purple) and compound **14c** (blue) docked in the ATP binding site of EGFR PTK, showing perfect overlay of the quinazoline ring in lapatinib and 2-benzoyl moiety in **14c** (for interpretation of the references to colour in this figure legend, the reader is referred to the web version of this article).

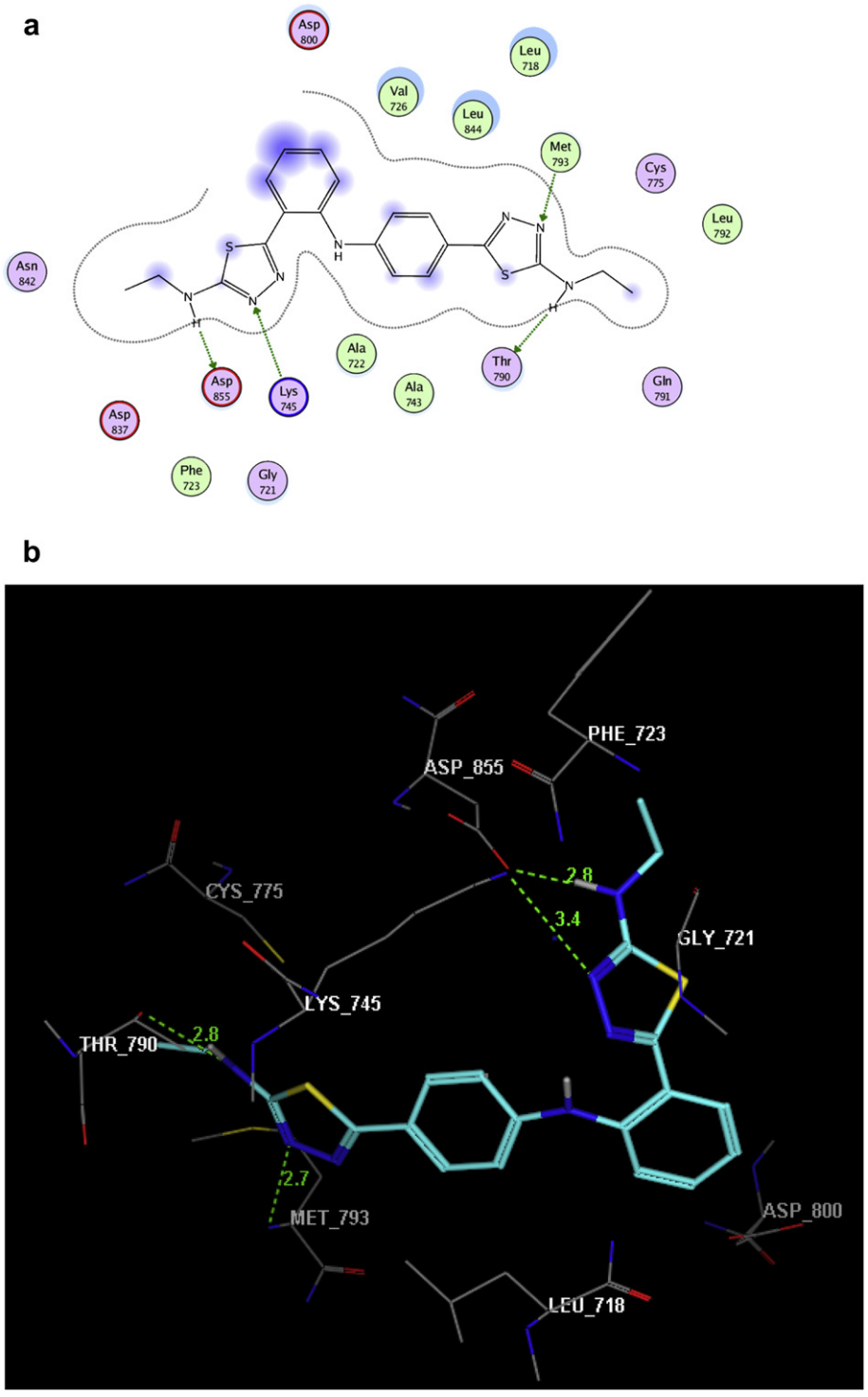

Fig. 5. Docking of compound **16a** in the ATP binding site of EGFR PTK in 2D diagram (a) and in 3D style (b).

are given as percentage inhibition at concentration of 10 μM of the inhibitor.

The results showed that, for a series of 2,4′-bis-(*N*-substituted) diphenylamine hydrazones **14a**–**g**, only the arylidene analogues with lipophilic electron-donating group on the benzylidene moiety showed moderate inhibitory activity. e.g. **14c** and **14e** resulted in 47% and 50% inhibition, respectively. The unsubstituted analogue **14a**, the 2-OH derivative **14b** and the 4-Cl derivative **14d** were inactive. Also, a similar behavior has been noted on replacement of the aryl moiety with furan **14f** or 5-nitrofuran **14g**, probably due to the electron-withdrawing property of the furan ring.

In the 2,4′-bis-aminothiadiazole series **16a**–**c**, it was found that the substituent on amino greatly affects the kinase inhibitory activity. The *N*-ethyl analogue **16a** was a potent EGFR PTK inhibitor (98% inhibition). However, the activity was abolished if a phenyl or allyl group was attached to the amino (**16b** and **16c**). This proves poor bulk tolerance at this class of compounds. A similar trend was observed with respect to N-4 substitution of the triazole ring in the

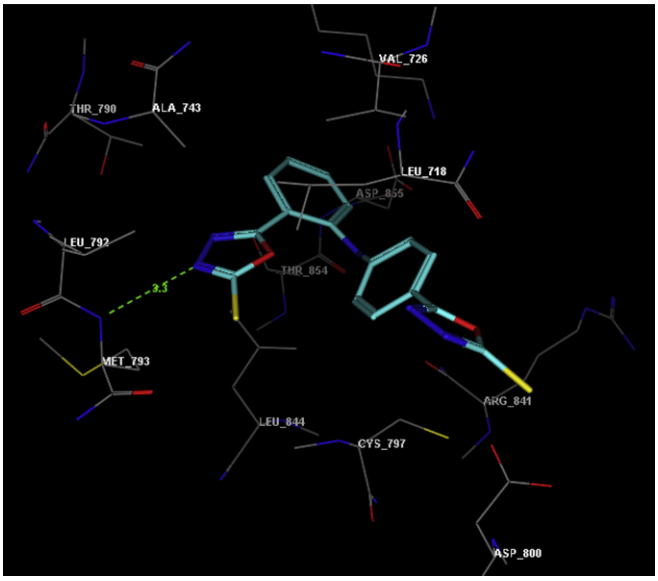

Fig. 6. Docking of compound **19** in the ATP binding site of EGFR PTK in 3D style.

2,4′-bis-5-mercapto-1,2,4-triazole series **17a**–**c**. The utility of small lipophilic ethyl group in **17a** resulted in 52% inhibition. Increasing the size of N-4 substituent on the triazole vanquished the activity in **17b** and **17c**. Also, changing the ethyl in **17a** with small hydrophilic amino function in **18** destroyed the enzyme inhibitory activity. The bis-5-mercapto-1,3,4-oxadiazole derivative **19** revealed 48% inhibition. Appending benzyl (**20b**) or allyl (**20c**) at 5-SH in **19** produced slight increase in the kinase inhibition. Interestingly, adding an ethyl group as in **20a** dramatically decreased the inhibitory potency against EGFR PTK.

3.2. In vitro cytotoxicity

Compounds **14c**, **14e**, **16a**, **17a**, **19**, **20b** and **20c** that showed EGFR inhibitory activity were evaluated for their antiproliferative activity on human breast cancer cell line (MCF-7) by Skehan's method [35]. MCF-7 is known to over-express EGFR and provides a good measure to determine the effectiveness of EGFR-TK inhibition. The IC_{50} of the tested compounds in μM are presented in Table 2.

The results indicate that, the 2,4′-bis-(*N*-substituted)diphenylamine hydrazones **14c** and **14e** were potent antiproliferative agents (IC_{50} 0.81 and 1.23 μM, respectively). The most potent EGFR inhibitor **16a** showed remarkable antitumor activity (IC_{50} = 0.94 μM). The replacement of the 5-ethylamino-1,3,4-thiadiazole moiety in **16a** with 4-ethyl-5-mercopto-1,2,4-triazole moiety in **17a** or 5-mercapto-1,3,4-oxadiazole moiety in **19** led to two fold decrease in activity. It is worth to note that both compounds possess free polar SH group that might lead to decreased cellular penetration. The elaboration of the 5-mercapto in **19** with allyl in **20c** resulted in two fold increase of activity, while substitution with the more lipophilic benzyl moiety produced the most active antiproliferative agent **20b** (IC_{50} = 0.73 μM).

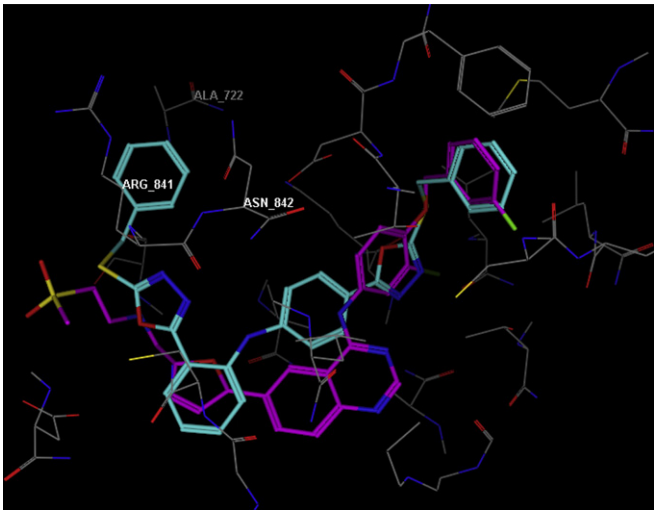

Fig. 7. The superposition of lapatinib (purple) and compound **20b** (blue) docked in the ATP binding site of EGFR PTK in 3D style (for interpretation of the references to colour in this figure legend, the reader is referred to the web version of this article).

3.3. Molecular modeling

To rationalize the obtained biological results and to describe the binding mode of the active compounds with their predicted intracellular target, docking analysis was carried out. Docking of the inhibitors into the crystal structure of EGFR kinase domain with lapatinib (PDB ID code 1XKK) [36] were performed using Molecular Operating Environment MOE version 2008.10 [37]. The X-ray crystal structure illustrates that lapatinib binds to the ATP binding cleft, where the quinazoline ring binds to the narrow hydrophobic pocket in the N-terminal of EGFR-TK, which is the binding site of the adenine base of ATP. The N-1 of the quinazoline ring is hydrogen bonded to the main chain NH of Met 793 whereas the N-3 makes water mediated hydrogen bond to the side chain of Thr 854. The 3′-chloro-4-[(3-fluorobenzyl)oxy]aniline lies in a deep hydrophobic pocket at the back of the ATP binding site [36]. In consistency with the design rational, docking of the hydrazone derivative **14c** showed that the benzoyl group of 2-benzohydrazide moiety binds in the adenine binding pocket and mimics the quinazoline ring of lapatinib, but with no possibility of intramolecular hydrogen bonding (Fig. 4). Both the carbonyl oxygen and NH of the hydrazide function are involved in water bridged hydrogen bond with Thr 854. The 2-(3,4-dimethoxybenzylidene)hydrazine is deeply oriented in the hydrophobic pocket occupied by the 3′-chloro-4-[(3-fluorobenzyl)oxy]aniline moiety of lapatinib. The 4′-(3,4-dimethoxybenzylidene)benzohydrazide is directed toward the entrance of the active site, where 3,4-dimethoxybenzylidene is positioned in a secondary pocket made of Ala 722, Arg 841 and Asn 842. It is worthy to note that, the extra hydrophobic interaction provide by para and meta methoxy groups in **14c** and the para dimethyl amino substituent in **14e** allowed more deep interaction with the hydrophobic pocket at the back of ATP binding site and more perfect fitting of the benzoyl moiety in the adenine binding pocket compared to the inactive hydrazone analogues **14a**, **b**, **d**, **f** and **g**.

Due to geometry and structural difference between the hydrazones **14** and the 2,4′-bis-heterocyclic diphenylamines **16**–**20**[1], the latter compounds were expected to adopt a slightly different binding mode. The details of interaction between the protein and the most potent 2,4′-bis-aminothiadiazole derivative **16a** are shown in Fig. 5a–b. The model reveals that, the 4′-(5-ethylamino-1,3,4-thiadiazol-2-yl)phenyl moiety binds the adenine binding pocket. The thiadiazole ring nitrogen N-4 interact with the

[1] To facilitate the interpretation of docking results, compounds 16–20 are considered as derivatives of 2,4′-bis substituted diphenylamine regardless of the IUPAC nomenclature adopted in the experimental part.

backbone NH of Met 793 via hydrogen bond (2.7 Å) and the 5-ethylamino NH is engaged in a second hydrogen bond with the side chain OH of Thr 790 (2.8 Å). The ethyl group is projecting in this narrow pocket near by Thr 790 side chain (Fig. 5b). This may explain the lack of activity of the phenyl and allyl analogues **16b** and **16c**. The steric clash caused by such bulky groups pushed the thiadiazole ring away leading to loss of the key hydrogen bond with Met 793. Hydrogen bonding with this amino acid helps to fix the adenine base of ATP in the binding pocket and is considered crucial for the activity of the classical quinazoline inhibitors [27,36]. Moreover, the 2-(5-ethylamino-1,3,4-thiadiazol-2-yl)phenyl is facing the entrance of the pocket with the phenyl is extended to the solvent exposed region. The thiadiazole N-4 and the ethylamino NH are involved in H-bonding with the side chain of Lys 745 and Asp 855 (3.4 Å and 2.8 Å respectively).

Docking of 2,4′-bis-5-mercaptotriazoles **17a**–**c** showed almost similar orientations and binding behavior. On the other hand compounds **18** and **19** revealed a backward orientation. It should be mentioned that hydrogen bonding with Met 793 residue can only be observed with the active analogues **17a** and **19** (Fig. 6).

The 2,4′-bis-1,3,4-oxadiazle series **20a**–**c** illustrates good bulk tolerance. This leads to the suggestion that, these molecules could interact deeply in the back of ATP binding site similar to lapatinib. The additional binding energy provided by the binding of the benzyl and allyl substituents in **20b** and **20c** in this deep pocket may be the reason for the high binding affinity of these molecules. Fig. 7 represents the superposition of the binding of lapatinib and **20b**. The 4′-[5-(benzylthio)-1,3,4-oxadiazol-2-yl] in **20b** is located in the back of the ATP binding site and makes predominant hydrophobic interaction with the protein mimicking the 3′-chloro-4-[(3-fluoro-benzyl)oxy]aniline in lapatinib. Moreover, the other benzyl group is involved in arene–arene interaction with Arg 841 side chain. In comparison, the much less potent analogue **20a** does not project deep in the pocket and binds near the entrance of the active site making fewer hydrophobic contacts.

4. Conclusion

This study reported the synthesis of 2,4′-(bis substituted) diphenylamine derivatives as a novel class of EGFR PTK inhibitors. Derivatives **14c**, **14e**, **16a**, **17a**, **19**, **20b** and **20c** exhibited promising enzyme inhibitory activity. The most active compound was **16a** that revealed 98% inhibition at concentration of 10 μM. SAR was discussed in terms of the enzyme inhibitory activity and was supported by docking studies and analysis of the binding mode of the new compounds. The electronic factor seem to be the most crucial factor affecting the activity of a series of 2,4′-bis-(*N*-substituted) diphenylamine hydrazones **14a**–**g**. Meanwhile, the steric effect seems to be the most important factor affecting the activity of 2,4′-bis-heterocyclic diphenylamines **16**–**20**. On the other hand, cytotoxicity results indicate that all evaluated compounds showed potent antitumor activity, IC_{50} ranging from 0.73 (**20b**) to 2.38 μM (**17a**). There is no definite relationship was found between the enzyme inhibitory activity and cellular efficiency, which suggests that this class of compounds might function by inhibiting multiple key proteins involved in the EGFR signaling pathways, not only targeting the tyrosine kinase. Thus, the new compounds led to significant antiproliferative effect against EGFR dependent tumor cell line, which over-express EGFR. The definite mechanism is to be investigated.

In summary, the newly synthesized compounds provide a promising new template for further development of potent EGFR inhibitors.

5. Experimental

5.1. Chemistry

Melting points were determined on a Gallenkamp melting point apparatus and are uncorrected. ^{1}H NMR spectra were recorded in DMSO-d_6, either on Varian XL-300 MHz or Jeol FX 90Q-90 MHz spectrometer (chemical shifts are given in parts per million PPM). ^{13}C NMR spectra were scanned on Varian XL-300 MHz spectrometer. The IR spectra were measured as potassium bromide pellets using a Pruker-FT IR spectrophotometer or Schimadzu IR spectrophotometer. Mass spectra were obtained at Fennigan MAT, SSQ 7000 spectrophotometer at 70 eV. Microanalytical data (C, H, N) of the synthesized compounds are within ±0.4 of the calculated values. Elemental analysis was carried out at the Microanalytical Unit, Faculty of Science, Cairo University. The intermediate 2, 4′-dipenylamine dicarboxylic acid **11** was prepared by reported procedure [32].

5.1.1. 2-{[4-(Methoxycarbonyl)phenyl]amino}benzoic acid methyl ester (*12*)

To an ice cold, stirred solution of **11** (3.9 mmol) in methanol (20 ml), thionyl chloride (1 ml) was added dropwise. Stirring was continued for 20 min at room temperature. The reaction mixture was heated under reflux for 4 h, then concentrated and left to cool. The crystalline product was filtered to give 0.85 g (77%). The product was recrystallized from ethanol, m.p. 74–75 °C. IR (KBr, ν cm^{-1}) 3300 (NH), 2950, 2900 (CH_3)s, 1720 (C=O)s. ^{1}H NMR (DMSO-d_6) δ (ppm) 3.81 (s, 3H, $\underline{CH_3}$), 3.83 (s, 3H, $\underline{CH_3}$), 7.00–7.93 (m, 8H, Ar-$\underline{H}$), 9.39 (s, 1H, NH, D_2O exchangeable). Anal. Calc. for $C_{16}H_{15}NO_4$: C, 67.36; H, 5.30; N, 4.91. Found C, 67.40; H, 5.16; N, 4.98.

5.1.2. 2-[4-(Hydrazinecarbonyl)phenylamino]benzoic acid hydrazide (*13*)

A mixture of **12** (3.5 mmol) and hydrazine hydrate (10 ml) was heated under reflux for 6 h, then concentrated under reduced pressure. After cooling the separated solid was filtered, washed with ethanol and dried to give 0.73 g (72%). The product was recrystallized from DMF, m.p. 245–247 °C. IR (KBr, ν cm^{-1}) 3289 (NH), 3219, 3182 (NH + NH_2)s, 1663 (C=O)s. ^{1}H NMR (DMSO-d_6) δ (ppm) 6.87–7.81 (m, 8H, Ar-$\underline{H}$), 9.38 (s, 1H, NH, D_2O exchangeable), 9.57 (s, 4H, $NH\underline{NH_2}$, D_2O exchangeable), 9.93 (s, 2H, $\underline{NH}NH_2$, D_2O exchangeable). Anal. Calc. for $C_{14}H_{15}N_5O_2$: C, 58.94; H, 5.30; N, 24.55. Found: C, 59.10; H, 5.01; N, 24.32.

5.1.3. General procedure for the synthesis of compounds (*14*)

To a refluxing solution of **13** (1.7 mmol) and the appropriate aldehyde (3.5 mmol) in absolute ethanol, 1 ml glacial acetic acid was added. The reaction mixture was heated under reflux for 4 h, then concentrated. After cooling, the separated solid was filtered and washed with ethanol. The crude product was recrystallized from the appropriate solvent.

*5.1.3.1. 2,4′-Azanediylbis(N′-benzylidenebenzohydrazide) (**14a**).* Recrystallization from ethanol (yield 95%), m.p. 260–262 °C. IR (KBr, ν cm^{-1}) 3359, 3216 (NH)s, 3032 (aromatic CH), 1635 (C=O) s. ^{1}H NMR (DMSO-d_6) δ (ppm) 6.70–7.67 (m, 18H, Ar-$\underline{H}$), 8.39 (s, 2H, 2× –N=$\underline{CH}$), 9.30 (s, NH), 11.68 and 11.90 (s, 2× CO$\underline{NH}$ cis and trans conformers). Anal. Calc. for $C_{28}H_{23}N_5O_2$: C, 72.87; H, 5.02; N, 15.1. Found: C, 72.81; H, 4.82; N, 15.23.

*5.1.3.2. 2,4′-Azanediylbis[N′-(2-hydroxybenzylidene)benzohydrazide] (**14b**).* Recrystallization from DMF/H_2O (yield 95%), m.p. 212–214 °C. IR (KBr, ν cm^{-1}) 3400, 3350 (OH)s, 3200 (NH)s, 1640,1620 (C=O)s. ^{1}H NMR (DMSO-*d*6) δ (ppm) 6.89–7.91 (m, 16H,

Ar-H), 8.60 (s, 2H, 2× –N=CH), 9.41 (s, NH, D_2O exchangeable), 11.24 and 11.42 (s, 2× CONH cis and trans conformers, D_2O exchangeable), 11.95 and 12.15 (s, 2× OH, D_2O exchangeable). Mass (%): M^+ 493 (12.75). Anal. Calc. for $C_{28}H_{23}N_5O_4.2H_2O$: C, 63.51; H, 5.14; N, 13.23. Found: C, 63.39; H, 5.37; N, 13.05.

*5.1.3.3. 2,4′-Azanediylbis[N′-(3,4-dimethoxybenzylidene)benzohydrazide] (**14c**).* Recrystallization from DMF (yield 92%), m.p >300 °C. IR (KBr, ν cm^{-1}) 3313, 3184 (NH)s, 3001 (aromatic CH), 1636 (C=O)s. ^1H NMR (DMSO-d_6) δ (ppm) 3.73 and 3.82 (s, 12H, 4× OCH_3), 6.97–7.82 (m, 14H, Ar-H), 8.32 (s, 2H, 2× –N=CH), 9.38 (s, NH), 11.64 and 11.86 (s, 2× CONH cis and trans conformers). Anal. Calc. for $C_{32}H_{31}N_5O_6$: C, 66.08; H, 5.37; N, 12.04. Found: C, 66.13; H, 5.06; N, 11.93.

*5.1.3.4. 2,4′-Azanediylbis[N′-(4-chlorobenzylidene)benzohydrazide] (**14d**).* Recrystallization from DMF/H_2O (yield 83%), m.p. 270–272 °C. IR (KBr, ν cm^{-1}) 3200 (NH)s, 3050 (aromatic CH), 1650 (C=O)s, 750 (C–Cl). ^1H NMR (DMSO-d_6) δ (ppm) 7.10–7.87 (m, 16H, Ar-H), 8.40 and 8.70 (s, 2H, 2× –N=CH cis and trans conformers), 9.57 (s, NH), 11.90 and 12.10 (s, 2× CONH cis and trans conformers). Anal. Calc. for $C_{28}H_{21}Cl_2N_5O_2$: C, 63.40; H, 3.99; N, 13.37. Found: C, 63.41; H, 4.26; N, 13.20.

*5.1.3.5. 2,4′-Azanediylbis{N′-[4-(dimethylamino)benzylidene]benzohydrazide} (**14e**).* Recrystallization from DMF/H_2O (yield 93%), m.p. 224–226 °C. IR (KBr, ν cm^{-1}) 3200 (NH)s, 3050 (aromatic CH), 2900 (aliphatic CH), 1640,1650 (C=O)s. ^1H NMR (DMSO-d_6) δ (ppm) 2.97 (s, 12H, 4× CH_3), 6.70–7.58 (m, 16H, Ar-H), 8.27 and 8.51 (s, 2H, 2× –N=CH cis and trans conformers), 9.40 (s, NH), 11.40 and 11.66 (s, 2× CONH cis and trans conformers). Anal. Calc. for $C_{32}H_{33}N_7O_2$: C, 70.18; H, 6.07; N, 17.90. Found: C, 70.06; H, 6.28; N, 17.96.

*5.1.3.6. 2,4′-Azanediylbis[N′-(furan-2-ylmethylene)benzohydrazide] (**14f**).* Recrystallization from DMF/H_2O (yield 78%), m.p. 246–248 °C. IR (KBr, ν cm^{-1}) 3200 (NH)s, 3050 (aromatic CH), 1640,1650 (C=O)s. ^1H NMR (DMSO-d_6) δ (ppm) 6.63–7.83 (14H, m, Ar-H + furan protons), 8.28 (s, 2H, 2× –N=CH), 9.31 (s, NH), 11.65 and 11.88 (s, 2× CONH cis and trans conformers). Anal. Calc. for $C_{24}H_{19}N_5O_4$: C, 65.30; H, 4.34; N, 15.86. Found: C, 65.02; H, 4.62; N, 15.70.

*5.1.3.7. 2,4′-Azanediylbis{N′-[(5-nitrofuran-2-yl)methylene]benzohydrazide} (**14g**).* Recrystallization from DMF/H_2O (yield 70%), m.p. 288–290 °C. IR (KBr, ν cm^{-1}) 3320,3227 (NH)s, 3060 (aromatic CH), 1647 (C=O)s. ^1H NMR (DMSO-d_6) δ (ppm) 7.11–7.84 (m, 12H, Ar-H + furan protons), 8.39 (s, 2H, 2× –N=CH), 9.31 (s, NH), 12.04 and 12.30 (s, 2× CONH cis and trans conformers). Anal. Calc. for $C_{24}H_{17}N_7O_8$: C, 54.24; H, 3.22; N, 18.45. Found: C, 54.15; H, 3.51; N, 18.36.

*5.1.4. General procedure for the synthesis of compounds (**15**)*

A mixture of the acid hydrazide **13** (1.0 mmol) and the appropriate isothiocyanate (3.0 mmol) was refluxed in absolute ethanol for 8 h the reaction mixture was concentrated and left to cool. The separated solid was filtered and recrystallized from the appropriate solvent.

*5.1.4.1. N-Ethyl-2-{2-[4-(2-(ethylcarbamothioyl)hydrazinecarbonyl)-phenylamino]benzoyl}hydrazinecarbothioamide (**15a**).* Recrystallization from DMF/H_2O (yield 85%), m.p. 220–222 °C. IR (KBr, ν cm^{-1}) 3250, 3177 (NH)s, 2969 (C–H), 1647 (C=O)s, 1254 (C=S)s. ^1H NMR (DMSO-d_6) δ (ppm) 1.04–1.09 (t, 6H, 2× CH_2CH_3), 3.45–3.49 (q, 4H, 2× CH_2CH_3), 6.98–7.87 (m, 8H, Ar-H), 8.01–8.06 (d, 2× NHCH$_2$CH$_3$, D_2O exchangeable), 9,14–9.19 (d, 2×, NHC=S, D_2O exchangeable), 9.6 (s, NH, D_2O exchangeable), 10.11 and 10.37 (s, 2×, CONH, D_2O exchangeable). Anal. Calc. for $C_{20}H_{25}N_7O_2S_2$: C, 52.27; H, 5.48; N, 21.33. Found: 52.68; 4.83; 21.33.

*5.1.4.2. N-Phenyl-2-{2-[4-(2-(phenylcarbamothioyl)hydrazinecarbonyl)- phenylamino]benzoyl}hydrazinecarbothioamide (**15b**).* Recrystallization from ethanol (yield 76%), m.p. 162-4 °C. IR (KBr, ν cm^{-1}) 3238 (NH)s, 3059 (aromatic CH), 1656 (C=O)s, 1254 (C=S)s. ^1H NMR (DMSO-d_6) δ (ppm) 7.17–7.91 (18H, m, Ar-H), 9.52 (s, NH), 9.76 (d, 2× NHph and 2× NHC = S), 10.33 and 10.60 (s, 2× CONH). ^{13}C NMR (DMSO-d_6) δ 116.79, 119.66, 120.68, 124.52, 125.07, 127.99, 129.55,132.45, 139.10 (C–NHC=S), 139.26 (C–NHC=S), 145.16 (C–NH), 149.48 (C–NH), 165.51 (C=O), 181.38 (C=S). Mass (%): M-1 554 (4.26). Anal. Calc. for $C_{28}H_{25}N_7O_2S_2$: C, 60.52; H, 4.53; N, 17.64. Found: C, 60.24; H, 4.61; N, 17.64.

*5.1.4.3. N-Allyl-2-{2-[4-(2-(allylcarbamothioyl)hydrazinecarbonyl)-phenylamino]benzoyl}hydrazinecarbothioamide (**15c**).* Recrystallization from DMF/H_2O (yield 90%), m.p. 214–216 °C. IR (KBr, ν cm^{-1}) 3251, 3167 (NH)s, 1648 (C=O)s, 1258 (C=S)s. ^1H NMR (DMSO-d_6) δ (ppm) 4.05 (d, 4H, 2× –CH_2–CH=CH_2), 4.89 (d, 4H, 2× –CH_2–CH=CH_2), 5.6–6.00 (m, 2H, 2× –CH_2–CH=CH_2), 7.15–7.81 (m, 8H, Ar-H), 8.30 (s, 2× NH-allyl), 9.3 (s, 2× NHC=S), 9.60 (s, NH), 10.18 and 10.60 (s, 2×, CONH). Anal. Calc. for $C_{22}H_{25}N_7O_2S_2$: C, 54.64; H, 5.21; N, 20.27. Found: C, 54.33; H, 5.00; N, 20.10.

*5.1.5. General procedure for the synthesis of compounds (**16**)*

A suspension of the appropriate thiosemicarbazide **15** (1.0 mmol) in 2 equivalent amount of freshly prepared PPA solution was stirred at room temperature till homogenous, then for 1 h at 110 °C. The reaction mixture was cooled, then poured over crushed ice. The precipitated product was filtered, washed with water and crystallized from an appropriate solvent.

*5.1.5.1. N-Ethyl-5-{2-[4-(5-(ethylamino)-1,3,4-thiadiazol-2-yl)phenylamino]-phenyl}-1,3,4-thiadiazol-2-amine (**16a**).* Recrystallization from DMF/ethanol (yield 75%), m.p. 150–152 °C. IR (KBr, ν cm^{-1}) 3267 (NH)s, 2972 (C_2H_5)s, 1589 (C=N)s. ^1H NMR (DMSO-d_6) δ (ppm) 1.04–1.18 (t, 3H, CH_2CH_3), 1.22–1.23 (t, 3H, CH_2CH_3), 3.31–3.34 (q, 2H, CH_2CH_3) 3.42–3.51 (m, 2H, CH_2CH_3, overlaped), 6.93–7.84 (m, 8H, Ar-H), 9.19 (s, NH), 10.36 (s, 2× NHCH$_2$CH$_3$). ^{13}C NMR (DMSO-d_6) δ 14.14 (CH_3), 14.39 (CH_3), 38.52 (CH_2), 116.52, 118.28, 119.25, 120.63, 123.19, 127.63, 129.58, 132.39, 143.28 (C–NH), 155.61 (C=N), 167.48 (C=N). Mass (%): M^+ 423 (75.50). Anal. Calc. for $C_{20}H_{21}N_7S_2$: C, 56.71; H, 5.00; N, 23.15; Found C, 56.56; H, 4.72; N, 23.15.

*5.1.5.2. N-Phenyl-5-{2-[4-(5-(phenylamino)-1,3,4-thiadiazol-2-yl) phenylamino]-pheny})-1,3,4-thiadiazol-2-amine (**16b**).* Recrystallization from DMF/ethanol (yield 65%), m.p. 178–180 °C. IR (KBr, ν cm^{-1}) 3275 (NH)s, 3029 (aromatic CH), 1594 (C=N)s. ^1H NMR (DMSO-d_6) δ (ppm) 7.26–8.41 (m, 18H, Ar-H), 8.60 (s. NH), 11.96 (s, 2× NH-ph). Anal. Calc. for $C_{28}H_{21}N_7S_2$: C, 64.72; H, 4.07; N, 18.87; Found C, 64.55; H, 3.86; N, 18.73.

*5.1.5.3. N-Allyl-5-{2-[4-(5-(allylamino)-1,3,4-thiadiazol-2-yl)phenylamino]-phenyl}-1,3,4-thiadiazol-2-amine (**16c**).* Recrystallization from DMSO (yield 81%), m.p. 167–169 °C. IR (KBr, ν cm^{-1}) 3271 (NH)s, 1589 (C=N)s. ^1H NMR not done due to solubility problems. Anal. Calc. for $C_{22}H_{21}N_7S_2$: C, 59.04; H, 4.73; N, 21.91. Found: C, 59.25; H, 4.56; N, 21.95.

*5.1.6. General procedure for the synthesis of compounds (**17**)*

A solution of appropriate thiosemicarbazide **15** (1.0 mmol) in 2 N NaOH was refluxed for 3 h. The resulting solution was filtered.

The filtrate was cooled and acidified with dilute HCl to pH = 5–6. The precipitate formed was filtered, washed with water and crystallized from an appropriate solvent.

*5.1.6.1. 4-Ethyl-3-{2-[4-(4-ethyl-5-thioxo-4,5-dihydro-1H-1,2,4-triazol-3-yl)phenylamino]phenyl}-1H-1,2,4-triazole-5(4H)-thione (**17a**).* Recrystallization from aqueous ethanol (yield 93%), m.p. 223–225 °C. IR (KBr, ν cm^{-1}) 3308 (NH), 3084 (aromatic CH), 2933 (C_2H_5)s, 2747 (w, SHs), 1608 (C=N)s. ^{1}H NMR (DMSO-d_6) δ (ppm) 1.01–1.05 and 1.15–1.21 (t, 3H, 2× $CH_2\underline{CH_3}$), 3.76–3.80 and 4.02–4.05 (q, 2H, 2× $\underline{CH_2}CH_3$), 7.10–7.53 (m, 8H, Ar-H), 8.23 (s, NH, D_2O exchangeable), 13.78 and 13.81 (s, 2×, thioxotriazole $\underline{NH}$, D_2O exchangeable). Mass (%): M^+ 423 (85.65). Anal. Calc. for $C_{20}H_{21}N_7S_2$: C, 56.71; H, 5.00; N, 23.15; Found C, 56.90; H, 4.90; N, 23.08.

*5.1.6.2. 4-Phenyl-3-{2-[4-(4-phenyl-5-thioxo-4,5-dihydro-1H-1,2,4-triazol-3-yl)-phenylamino]phenyl}-1H-1,2,4-triazole-5(4H)-thione (**17b**).* Recrystallization from aqueous ethanol (yield 83%), m.p. 192–194 °C. IR (KBr, ν cm^{-1}) 3200 (NH), 3064 (aromatic CH), 2741 (w, SHs), 1591 (C=N)s. ^{1}H NMR (DMSO-d_6) δ (ppm) 6.44–7.60 (m,18H, Ar-$\underline{H}$), 8.03 (s, $\underline{NH}$), 13.94 and 14.08 (s, 2× thioxotriazole $\underline{NH}$). ^{13}C NMR (DMSO-d_6) δ 115.14, 116.15, 117.15, 119.63, 120.64, 121.64, 127.39,128.09, 128.34, 128.77, 129.29, 131.29, 132.23, 133.74 (C–N), 134.58 (C–N), 140.52 (C–NH), 144.93 (C–NH), 149.53 (C-3 thioxotriazole), 150.73 (C-3 thioxotriazole), 167.62 (C-5 thioxotriazole), 168.24 (C-5 thioxotriazole). Anal. Calc. for $C_{28}H_{21}N_7S_2$: C, 64.72; H, 4.07; N, 18.87; Found C, 64.50; H, 3.92; N, 18.85.

*5.1.6.3. 4-Allyl-3-{2-[4-(4-allyl-5-thioxo-4,5-dihydro-1H-1,2,4-triazol-3-yl)phenylamino]phenyl}-1H-1,2,4-triazole-5(4H)-thione (**17c**).* Recrystallization from aqueous ethanol (yield 95%), m.p. 129–131 °C. IR (KBr, ν cm^{-1}) 3358 (NH), 3096 (aromatic CH), 2750 (w, SHs), 1606 (C=N)s. ^{1}H NMR (DMSO-d_6) δ (ppm) 4.42 (d, 4H, 2× $\underline{CH_2}$–CH=CH_2), 4.66 (d, 4H, 2× CH_2–CH=$\underline{CH_2}$), 5.46–5.90 (m, 2H, 2× CH_2–$\underline{CH}$=CH_2), 7.03–7.46 (m, 8H, Ar-$\underline{H}$), 8.28 (s. NH), 13.90–13.93 (d, 2× thioxotriazole $\underline{NH}$). Anal. Calc. for $C_{22}H_{21}N_7S_2$: C, 59.04; H, 4.73; N, 21.91. Found: C, 59.40; H, 4.90; N, 21.85.

*5.1.7. 4-Amino-5-{2-[4-(4-amino-5-mercapto-4H-1,2,4-triazol-3-yl)phenylamino]-phenyl}-4H-1,2,4-triazole-3-thiol (**18**)*

To an ice-cooled mixture of the hydrazide **13** (10 mmol) and potassium hydroxide (30 mmol) in absolute ethanol (20 ml), carbon disulfide (12 ml) was added dropwise. After addition was complete, absolute ethanol (15 ml) was added and the reaction mixture was allowed to stir at room temperature overnight. After the addition of dry ether (50 ml), the obtained product was treated with hydrazine hydrate (99%; 40 mmol) and water (4 ml) and heated under reflux for 2 h. The reaction mixture was diluted with water and neutralized with concentrated hydrochloric acid. The separated solid was filtered, wash with water and recrystallized from ethanol (yield 95%), m.p. 160–162 °C. IR (KBr, ν cm^{-1}) 3300, 3153 (NH)s, 2749 (w, SH), 1594 (C=N)s. ^{1}H NMR (DMSO-d_6) δ (ppm) 5.67–5.74 (d, 2× NH_2, D_2O exchangeable), 7.03–7.73 (m, 8H, Ar-H), 8.32 (s, NH, D_2O exchangeable), 13.8 (s, br, 2× thioxotriazole $\underline{NH}$, D_2O exchangeable). Mass (%): M^+ 397 (0.25). Anal. Calc. for $C_{16}H_{15}N_9S_2$: C, 48.35; H, 3.80. Found: C, 48.70; H, 4.00.

*5.1.8. 5-{2-[4-(5-Mercapto-1,3,4-oxadiazol-2-yl)phenylamino] phenyl}-1,3,4-oxadiazole-2-thiol (**19**)*

To an ice-cooled mixture of the hydrazide **13** (10 mmol) and potassium hydroxide (20 mmol) in absolute ethanol (20 ml), carbon disulfide (100 mmol) was added dropwise. The reaction mixture was heated under reflux for 24 h, then distilled under vacuum. The residue was diluted with water and acidified with hydrochloric acid. The precipitated product was filtered, washed with water (yield 81%). The product was recrystallized from ethanol, m.p. 270–272 °C. IR (KBr, ν cm^{-1}) 3335 (NH), 2740 (w, SH), 1600 (C=N), 1173 (C–O–C). ^{1}H NMR (DMSO-d_6) δ (ppm) 7.15–7.81 (m, 8H, Ar-$\underline{H}$), 8.59 (s, NH, D_2O exchangeable), 14.60 (s, br, 2× thioxo-oxadiazole NH D_2O exchangeable). Mass (%): M^+ 369 (8.90) Anal. Calc. for $C_{16}H_{11}N_5O_2S_2$: C, 52.02; H, 3.00; N, 18.9. Found C, 52.30; H, 3.21; N, 18.72.

*5.1.9. General procedure for the synthesis of compounds (**20**)*

To a mixture of the mercapto-oxadiazole derivative **19** (2.5 mmol) and anhydrous potassium carbonate (10 mmol) in dry acetone, a solution of the appropriate alkyl halide (10 mmol) in dry acetone was added. The mixture was heated under reflux for 24 h, filtered while hot and the residue was washed with hot acetone. The combined filtrate and wash were evaporated under vacuum. The solid product was collected and washed with water.

*5.1.9.1. 2-[5-(Ethylthio)-1,3,4-oxadiazol-2-yl]-N-{4-[5-(ethylthio)-1,3,4-oxadiazol-2-yl]phenyl}aniline (**20a**).* Recrystallization from acetone (yield 90%), m.p. 124–126 °C. IR (KBr, ν cm^{-1}) 3295 (NH), 2969 (C_2H_5)s, 1602 (C=N), 1175 (C–O–C). ^{1}H NMR ($CDCl_3$) δ (ppm) 1.47–1.53 (t, 6H, 2× $CH_2\underline{CH_3}$), 3.25–3.34 (m, 4H, 2× $\underline{CH_2}CH_3$), 6.93–7.93 (m, 8H, Ar-$\underline{H}$), 9.44 (s, NH). ^{13}C NMR ($CDCl_3$) δ 14.69 (CH_3), 14.76 (CH_3), 27.05 (CH_2), 108.88, 115.49, 117.24, 119.65, 128.00, 128.34, 132.23, 141.86 (C–NH), 144.24 (C–NH), 163.47 (C-2 oxadiazole), 1644.97(C-5 oxadiazole), 165.50 (C-5 oxadiazole). Anal. Calc. for $C_{20}H_{19}N_5O_2S_2$: C, 56.45; H, 4.50; N, 16.46. Found: C, 56.50; H, 4.60; N, 16.54.

*5.1.9.2. 2-[5-(Benzylthio)-1,3,4-oxadiazol-2-yl]-N-{4-[5-(benzylthio)-1,3,4-oxadiazol-2-yl]phenyl}aniline (**20b**).* Recrystallization from acetone, (yield 85%), m.p. 138–140 °C. IR (KBr, ν cm^{-1}) 3303 (NH), 3063, 3030 (aromatic CH), 2978 (CH_2)s, 1594 (C=N), 1186 (C–O–C). ^{1}H NMR (DMSO-d_6) δ (ppm) 4.55 (s, 4H, 2× $\underline{CH_2}$), 7.11–7.86 (m, 18H, Ar-$\underline{H}$), 9.12 (s, NH D_2O exchangeable). Mass (%): M^+ 549 (19.30),. Anal. Calc. for $C_{30}H_{23}N_5O_2S_2$: C, 65.55; H, 4.22; N, 12.74. Found: C, 65.90; H, 4.50; N, 12.60.

*5.1.9.3. 2-[5-(Allylthio)-1,3,4-oxadiazol-2-yl]-N-{4-[5-(allylthio)-1,3,4-oxadiazol-2-yl]phenyl}aniline (**20c**).* Recrystallization from acetone (yield 85%), m.p. 90–92 °C. IR (KBr, ν cm^{-1}) 3289 (NH), 3072 (aromatic CH), 2977, 2934 (aliphatic CH), 1602 (C=N),1173 (C–O–C). ^{1}H NMR (DMSO-d_6) δ (ppm) 3.93–4.00 (d, 4H, 2× $\underline{CH_2}$–CH=CH_2), 5.24–5.44 (d, 4H, 2× CH_2–CH=$\underline{CH_2}$), 5.87–6.30 (m, 2H, 2× CH_2–$\underline{CH}$=CH_2), 7.28–7.91 (m, 8H, Ar-$\underline{H}$), 9.17 (s, NH). Anal. Calc. for $C_{22}H_{19}N_5O_2S_2$: C, 58.78; H, 4.26; N, 15.58. Found: C, 58.90; H, 4.10; N, 15.33.

5.2. In vitro EGFR inhibitory activity assays by ELISA

The assay was performed in 96-well plates pre-coated with 20 μg/mL Poly (Glu, Tyr) 4:1 (Sigma) as a substrate. In each well, 85 μL of 8 μM ATP solution and 100 μL of title compounds were added at 10 μM concentrations. PD153035 was used as a positive control for EGFR. The reaction was initiated by adding 5 μL of EGFR kinase. After incubation for 1 h at 37 °C, the plate was washed three times with PBS containing 0.1% Tween 20 (T-PBS). Next, 100 μL HRP-conjugate antiphospho-tyrosine antibody was added. After 1 h of incubation at room temperature, the plate was washed three times. TMB substrate solution (100 μL) diluted in T-PBS containing 5 mg/mL BSA was added. The plate was reincubated at room temperature (18–25 °C) for 15 min, and washed as before. The reaction was terminated by the addition of 100 μL of 1 M H_2SO_4, and A492 was measured using an ELISA reader. Results should be read immediately after addition of the stop solution.

The inhibition rate (%) was calculated using the equation: The inhibition % = [1 − (A492/A492 control)] × 100%

5.3. In vitro cytotoxic assay

The human tumor cell lines (MCF-7) were obtained as a gift from NCI, MD, USA. All chemicals and solvents were purchased from Sigma–Aldrich. The cytotoxic activity was measured in vitro using the Sulfo-Rhodamine-B stain (SRB) assay by the method of Skehan [35].

Cells were inoculated in 96-well microtiter plate (10^4 cells/well) for 24 h before treatment with the compound(s) to allow attachment of cell to the wall of the plate. Test compounds were dissolved in DMSO and diluted with saline to the appropriate volume. Different concentrations of the compound under test (0.1, 2.5, 5, and 10 nmol/ml) were added to the cell monolayer. Triplicate wells were prepared for each individual dose. Monolayer cells were incubated with the compound(s) for 48 h at 37 °C and in atmosphere of 5% CO_2. After 48 h, cells were fixed, washed, and stained for 30 min with 0.4% (w/v) SRB dissolved in 1% acetic acid. Unbound dye was removed by four washes with 1% acetic acid, and attached stain was recovered with Tris-EDTA buffer. Color intensity was measured in an ELISA reader. The relation between surviving fraction and drug concentration is plotted to get the survival curve for breast tumor cell line after the specified time. The concentration required for 50% inhibition of cell viability (IC_{50}) was calculated and the results are given in Table 2.

5.4. Molecular modeling

All molecular modeling calculation and docking studies were carried out using Molecular Operating Environment MOE version 2008.10 [37]. The target compounds were drawn on MOE. The structures were subjected to energy minimization using Hamiltonian-Force Field-MMFF94x and partial charges were calculated. The X-ray crystal structure of the kinase domain of EGFR in complex with GW572016 (lapatinib) PDB ID code 1XKK was recovered RSCB protein data bank [36]. The enzyme was prepared for docking as follows: (1) The Co-crystallized ligand, phosphate ions and water molecules outside the binding pocket were removed. (2) The enzyme was 3D protonated, where hydrogen atoms were added at their standard geometry, the partial charges were computed and the system was optimized. Flexible ligand − rigid receptor docking was done with MOE-DOCK using triangle matcher as placement method and affinity dG as a scoring function. The obtained poses were subjected to force field refinement using the same scoring function. 30 conformers of the ligand were retained with the highest and best score. In order to validate the docking procedure, lapatinib was docked into the active site of 1XKK. The docking results showed that the compound exhibited similar interaction to that reported in literature [36]. Ligand–receptor docking was demonstrated by 2D and 3D ligand–receptor interaction.

Acknowledgment

The author is grateful for Dr. Nadia Hamdy, Department of Biochemistry, Faculty of Pharmacy, Ain Shams University, for conducting the in vitro EGFR inhibitory activity assays. The author thanks the National Cancer Institute, Cairo University, for performing the in vitro cytotoxicity.

References

[1] M.A. Olayioye, R.M. Neve, H.A. Lane, N.E. Hynes, EMBO. J. 19 (2000) 3159–3167.
[2] Y. Yarden, Eur. J. Cancer 37 (2001) S3–S8.
[3] J. Baselga, C.L. Arteag, J. Clin. Oncol. 23 (2005) 2445–2459.
[4] A. Reid, L. Vidal, H. Shaw, J. De Bono, Eur. J. Cancer 43 (2007) 481–489.
[5] A.A. El-Zayat, T.F. Pingree, P.M. Mock, G.M. Clark, R.A. Otto, D.D. Von Hoff, Cancer J. 4 (1991) 375–380.
[6] J.R. Woodburn, Pharmacol. Ther. 82 (1999) 241–250.
[7] P. Traxler, Expert Opin. Ther. Targets 7 (2003) 215–234.
[8] J. Yi, L. Hui-Yuan, L. Li-ping, T. Jinzhi, D. jain, L. Xiaomin, L. Ya-Qiu, Bioorg. Med. Chem. 13 (2005) 5613–5622.
[9] F. Ciardiello, R. Caputo, R. Bianco, D. Vincenzo, G. Somatico, S. DePlacido, R. A. Bianco, G. Tortora, Clin. Cancer Res. 6 (2000) 2053–2063.
[10] R. Nahta, F.J. Esteva, Cancer Lett. 232 (2006) 123–138.
[11] N.I. Goldstein, M. Prewett, K. Zuklys, P. Rockwell, J. Mendelsohn, Clin. Cancer Res. 1 (1995) 1311–1318.
[12] K. Abouzid, S. Shouman, Bioorg. Med. Chem. 16 (2008) 7543–7551.
[13] D.W. Rusnak, K. Lackey, K. Affleck, E.R. Wood, K.J. Alligood, N. Rhodes, B. R. Keith, D.M. Murray, W.B. Knight, R.J. Mullin, T.M. Gilmer, Mol. Cancer Ther. 1 (2001) 85–94.
[14] W.A. Denny, Il Farmaco 56 (2001) 51–56.
[15] G.W. Rewcastle, W.A. Denny, A.L. Bridges, H. Zhou, D.R. Cody, A. McMichael, D. W. Fry, J. Med. Chem. 38 (1995) 3482–3487.
[16] A.A. San Jun, Eur. J. Med. Chem. 43 (2008) 781–791.
[17] R. Albuschat, W. Lowe, M. Weber, P. Luger, V. Jendrossek, Eur. J. Med. Chem. 39 (2004) 1001–1011.
[18] M.D. Gaul, Y. Guo, K. Affleck, G.S. Cockerill, T.M. Gilmer, R.J. Griffin, S. Guntrip, B. R. Keith, W.B. Knight, R.J. Mullin, D.M. Murray, D.W. rusnak, K. Smith, S. Tadepalli, E.R. Wood, K. Lackey, Bioorg. Med. Chem. Lett. 13 (2003) 637–640.
[19] J.J. Liao, J. Med. Chem. 50 (2007) 409–424.
[20] C.N. Hodge, J. Pierce, Bioorg. Med. Chem. Lett. 3 (1993) 1605–1608.
[21] P. Traxler, J. Green, H. mett, U. Sequin, P. Fure, J. Med. Chem. 42 (1999) 1018–1026.
[22] C. Liechti, U. Sequin, G. Bold, P. Furet, T. Meyer, P. Traxler, Eur. J. Med. Chem. 39 (2004) 11–26.
[23] G. Xu, L.L. Searle, T.V. Hughes, A.K. Beck, P.J. Connlly, M.C. Abad, M.P. Neeper, G.T. Struble, B.A. Springer, S.L. Emanuel, R.H. Gruninger, N. Pandey, M. Adams, S. Moreno-Mazza, A.R. Fuentes-Pesquera, S.A. Middleton, L.M. Greenberger, Bioorg. Med. Chem. Lett. 18 (2008) 3495–3499.
[24] G. Xu, M.C. Abad, P.J. Connlly, M.P. Neeper, G.T. Struble, B.A. Springer, S. L. Emanuel, N. Pandey, R.H. Gruninger, M. Adams, Moreno Mazza, A.R. Fuentes-Pesquera, S.A. Middleton, Bioorg. Med. Chem. Lett. 18 (2008) 4615–4619.
[25] T. Shimizu, Y. Fujiwara, T. Osawa, T. Sakai, K. Kubo, K. Kubo, T. Nishitoba, K. Kimura, T. Senga, H. Murooka, A. Iwai, K. Fukushima, T. Yoshino, A. Miwa, Bioorg. Med. Chem. Lett. 14 (2004) 875–879.
[26] G.W. Rewcastle, B.D. Palmer, A.L. Bridges, H.D. Hollis Showalter, L. Sun, J. M. Nelson, A. Mcmichael, A.J. Kraker, D.W. Fry, W.A. Denny, J. Med. Chem. 39 (1996) 918–928.
[27] B.D. Palmer, S.T. Kallmeyer, D.W. Fry, J.M. Nelson, H.D. Hollis Showalter, W. A. Denny, J. Med. Chem. 40 (1997) 1519–1529.
[28] N. Demirbas, A.U. Demirbas, Bioorg. Med. Chem. 10 (2002) 3717–3723.
[29] L. Jin, J. Chen, B. Song, Z. Chen, S. Yang, Q. Li, D. Hu, R. Xu, Bioorg. Med. Chem. Lett. 16 (2006) 5036–5040.
[30] M.S. Gujral, P.M. Patnaik, R. Kaul, H.K. Parikh, C. Conradt, C. Tamhankar, G. V. Daftary, Cancer Chemother. Pharmacol. 47 (2001) S23–S28.
[31] W. Rzeski, J. Matysiak, M. Kandefer-Szerszen, Bioorg. Med. Chem. 15 (2007) 3201–3207.
[32] I.B. Traporewala, J.M. Kuffman, J. Pharm. Sci. 79 (1990) 173–178.
[33] J.R. Reid, N.D. Heindel, J. Heterocyclic Chem. 13 (1976) 925–929.
[34] H.R. Tsou, N. Mamuya, B.D. Johnson, M.F. Reich, B.C. Gruber, F. Ye, R. Nilakantan, R. Shen, C. Discafani, R. DeBlanc, R. Davis, F.E. Koehn, L. M. Greenberger, Y.F. Wang, A. Wissner, J. Med. Chem. 44 (2001) 2719–2734.
[35] P. Skehan, R. Storeng, D. Scudiero, A. Monks, J. McMahon, D. Vistica, J. T. Warren, H. Bokesch, S. Kenney, M.R. Boyd, J. Natl. Cancer Inst. 82 (1990) 1107–1112.
[36] E.R. Wood, A.T. Truesdale, O.B. McDonald, D. Yuan, A. Hassell, S.H. Dickerson, B. Ellis, C. Pennisi, E. Horne, K. Lackey, K.J. Alligood, D.W. Rusnak, T.M. Gilmer, L. Shewchuk, Cancer Res. 64 (2004) 6652–6659.
[37] MOE. Chemical computing Group, Inc., Montereal http://www.chemcomp.com.